A New Fault Location Algorithm for Use With Current Differential Protective Relays of Series Compensated Transmission Lines

Murari Mohan Saha[1], Eugeniusz Rosolowski[2], Jan Izykowski[2]
[1] ABB AB, Sweden
[2] Wroclaw University of Technology, Poland
e-mail of contact author: murari.saha@se.abb.com

Abstract: An algorithm for locating faults on series-compensated transmission lines is presented. Use of two-end synchronized measurements of currents accomplished by current differential protective relays with additional incorporation of the locally measured three-phase voltage is considered. In case of double-circuit lines also providing of zero-sequence currents from the healthy parallel line is assumed. More superior solution with the fault location function embedded into the differential relays at both line ends is considered. The algorithm applies two subroutines designated for locating faults on line sections at both sides of the capacitor bank. Additionally the procedure for selecting the valid subroutine is applied. The developed algorithm has been tested and evaluated using signals taken from ATP-EMTP versatile simulations of faults on a test transmission line. The presented sample results of the testing show the validity of the presented fault location algorithm and its high accuracy.

Index Terms: transmission line, current differential protective relay, series capacitor compensation, measurement, fault location, fault simulation.

I. INTRODUCTION

When a fault occurs on an overhead line, it is very important for the utility to identify the fault location as precisely and quickly as possible for assuring the service reliability which became an important factor for network operators and customers. Algorithms for accurate location of faults on power lines are still a subject of great interest of researchers. Accurate fault location is especially of utmost importance for series-compensated lines [1]–[8], which are spreading over few hundreds of kilometers and are vital links between the energy production and consumption centers.

Among the known methods, the approach based on an impedance principle is the most popular. In particular, the algorithms utilizing one-end current and voltage measurements have been presented in [1]–[2]. In turn, in [3] use of two-end currents and voltages, measured synchronously with the aid of PMUs, has been considered. Use of the unsynchronized measurements has been proposed in [4]. The method for application with current differential protective relays of a single series-compensated line was introduced in [5]. The other fault location techniques for such lines are based on knowledge based approaches [6]–[7].

In this paper a new impedance-based fault location algorithm for series-compensated lines (Figs. 1 and 2) is presented. It is considered that a compensation is accomplished with fixed series capacitors (SCs) – Figs. 1 and 2. The SCs are equipped with MOVs (Metal Oxide Varistors) for overvoltage protection. The other details for the capacitor bank, as not important for the conducted considerations, are not shown in Figs. 1 and 2.

The approach from [5] was taken for further development and adaptation to get a novel fault location algorithm. The algorithm is formulated for a more general case of a double-circuit series compensated line (Fig. 2). Innovative contribution relies on using the following specific in-complete two-end measurements: – phasors $\{\underline{I}_{AA}\}$, $\{\underline{I}_{BA}\}$ of three-phase currents from both ends of the faulted line circuit measured by protective differential relays, – three-phase voltage $\{v_A\}$ measured locally, i.e.: at the bus AA, where the fault locator FL_A is consider as to be embedded into the relay $DIFF\_REL_A$, – zero-sequence current i_{AB0} from the healthy parallel line (provided for compensating for the mutual coupling between the line circuits).

The fault location function can be embedded into the differential relay at one end only [5] or into the relays at both line ends (Figs. 1 and 2). In the latter case much superior fault location is achieved and therefore it is taken for further considerations. The algorithm is derived for a double-circuit line (Fig. 2), however, after cancelling the mutual coupling elements it suits to a single line as well.

A fault is of a random nature and can appear at any line section, i.e. between the bus AA and the capacitor bank (fault F_A) or between the bus BA and the bank (fault F_B), as shown in Figs. 1 and 2.

Therefore, two subroutines: SUB_A (Section 2), SUB_B (Section 3) are utilized for locating these hypothetical faults F_A and F_B, respectively. The final result is selected with use of the selection unit described in Section 4. Section 5 is devoted to the evaluation of the presented fault location algorithm.

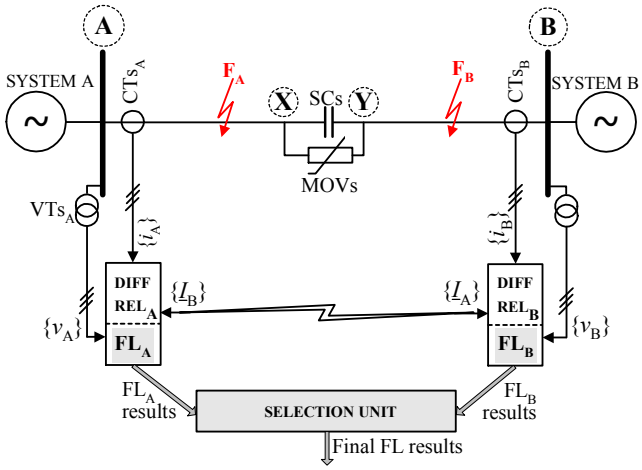

Fig. 1. Fault location with use of fault locators FL_A, FL_B embedded into the relays of a single series-compensated line

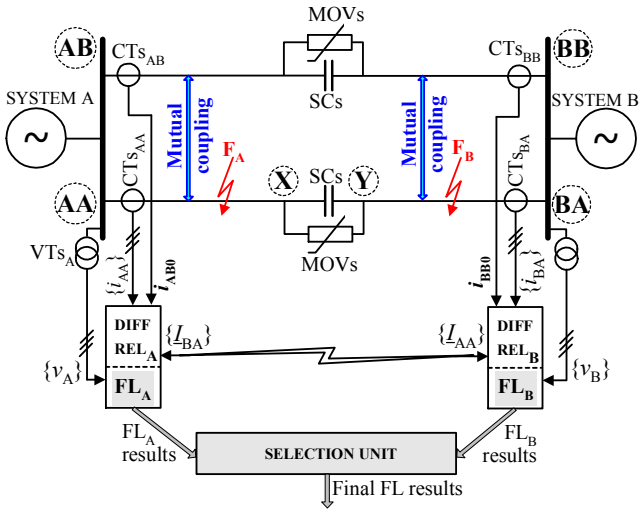

Fig. 2. Fault location with use of fault locators FL_A, FL_B embedded into the relays of a double-circuit series-compensated line

II. Fault Location Subroutine SUB_A

In relation to Fig. 3 the following generalized fault loop model [8] for fault FA can be stated:

$$\underline{V}_{Ap} - d_{FA}\underline{Z}_{1LA}\underline{I}_{Ap} - R_{FA}\underline{I}_{FA} = 0 \tag{1}$$

where: d_{FA} – unknown distance to fault [p.u.]; R_{FA} – unknown fault resistance; $\underline{V}_{Ap}$, $\underline{I}_{Ap}$ – fault loop voltage and current; $\underline{I}_{FA}$ – total fault current (fault path current); $\underline{Z}_{1LA}$ – positive-sequence impedance of the line section AA–X; Note: $\underline{Z}_{1LA} = d_{SC}\underline{Z}_{1L}$, where: $\underline{Z}_{1L}$ – positive-sequence impedance of the whole line AA–BA, d_{SC} – relative distance from bus AA to SCs&MOVs.

Fault loop voltage and current are composed accordingly to the fault type as follows [8]:

$$\underline{V}_{Ap} = \underline{a}_1\underline{V}_{A1} + \underline{a}_2\underline{V}_{A2} + \underline{a}_0\underline{V}_{A0} \tag{2}$$

$$\underline{I}_{Ap} = \underline{a}_1\underline{I}_{AA1} + \underline{a}_2\underline{I}_{AA2} + \underline{a}_0\left(\frac{\underline{Z}_{0LA}}{\underline{Z}_{1LA}}\underline{I}_{AA0} + \frac{\underline{Z}_{0mA}}{\underline{Z}_{1LA}}\underline{I}_{AB0}\right) \tag{3}$$

where: $\underline{a}_1$, $\underline{a}_2$, $\underline{a}_0$ – weighting coefficients (Table 1); 1, 2, 0 – digits in subscripts used for denoting positive-, negative- and zero-sequence components of the signals, $\underline{Z}_{0LA}$ – zero-sequence impedance of the line section AA–X, $\underline{Z}_{0mA}$ – zero-sequence mutual coupling impedance for the section AA–X.

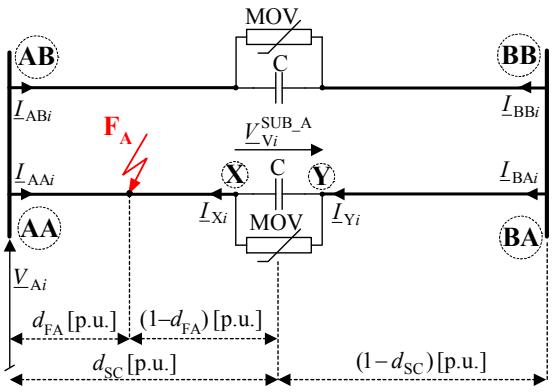

Fig. 3. Scheme for subroutine SUB_A (for fault FA)

Table 1. Weighting coefficients used in (2)–(3)

Fault type	$\underline{a}_1$	$\underline{a}_2$	$\underline{a}_0$
a-g	1	1	1
b-g	$-0.5-\mathrm{j}0.5\sqrt{3}$	$-0.5+\mathrm{j}0.5\sqrt{3}$	1
c-g	$-0.5+\mathrm{j}0.5\sqrt{3}$	$-0.5-\mathrm{j}0.5\sqrt{3}$	1
a-b, a-b-g a-b-c, a-b-c-g	$1.5+\mathrm{j}0.5\sqrt{3}$	$1.5-\mathrm{j}0.5\sqrt{3}$	0
b-c, b-c-g	$-\mathrm{j}\sqrt{3}$	$\mathrm{j}\sqrt{3}$	0
c-a, c-a-g	$-1.5+\mathrm{j}0.5\sqrt{3}$	$-1.5-\mathrm{j}0.5\sqrt{3}$	0

In order to minimize an influence of line shunt capacitances on accuracy of determining the total fault current involved in (1), it is not calculated by direct adding the phase currents at both ends of the faulted line. Instead, it is calculated using the following generalized fault model [8]:

$$\underline{I}_{FA} = \underline{a}_{F1}(\Delta\underline{I}_{AA1} + \Delta\underline{I}_{BA1}) + \underline{a}_{F2}(\underline{I}_{AA2} + \underline{I}_{BA2}) + \underline{a}_{F0}(\underline{I}_{AA0} + \underline{I}_{BA0}) \tag{4}$$

where: $\underline{a}_{F1}$, $\underline{a}_{F2}$, $\underline{a}_{F0}$ – share coefficients (Table 2); $\Delta\underline{I}_{AA1}$, $\underline{I}_{AA2}$, $\underline{I}_{AA0}$ – sequence components of currents at the bus AA; $\Delta\underline{I}_{BA1}$, $\underline{I}_{BA2}$, $\underline{I}_{BA0}$ – sequence components of currents at the bus BA.

Table 2. Share coefficients used in fault model (4)

Fault type	$\underline{a}_{F1}$	$\underline{a}_{F2}$	$\underline{a}_{F0}$
a-g	0	3	0
b-g	0	$-1.5+\mathrm{j}1.5\sqrt{3}$	0
c-g	0	$-1.5-\mathrm{j}1.5\sqrt{3}$	0
a-b	0	$1.5-\mathrm{j}0.5\sqrt{3}$	0
b-c	0	$\mathrm{j}\sqrt{3}$	0
c-a	0	$-1.5-\mathrm{j}0.5\sqrt{3}$	0
a-b-g	$1.5+\mathrm{j}0.5\sqrt{3}$	$1.5-\mathrm{j}0.5\sqrt{3}$	0
b-c-g	$-\mathrm{j}\sqrt{3}$	$\mathrm{j}\sqrt{3}$	0
c-a-g	$1.5-\mathrm{j}0.5\sqrt{3}$	$1.5+\mathrm{j}0.5\sqrt{3}$	0
a-b-c, a-b-c-g	$1.5+\mathrm{j}0.5\sqrt{3}$	$1.5-\mathrm{j}0.5\sqrt{3}$ *)	0
*) $\underline{a}_{F2} \neq 0$, however, negative-sequence component is not present			

Note that in (4) instead of using the fault quantities: $\underline{I}_{AA1}$, $\underline{I}_{BA1}$, the superimposed currents are applied:

$$\Delta\underline{I}_{AA1} = \underline{I}_{AA1} - \underline{I}^{pre}_{AA1}, \quad \Delta\underline{I}_{BA1} = \underline{I}_{BA1} - \underline{I}^{pre}_{BA1} \tag{5}$$

where the subtracted currents are taken from the pre-fault time interval (superscript: pre).

Usage of the superimposed quantities (5), and not the fault quantities, is advantageous since lower errors arise due to neglecting line shunt capacitances. The recommended share coefficients (Table 2) assures that the zero-sequence currents are not involved ($\underline{a}_{F0} = 0$) in total fault current calculations.

After resolving (3) into the real and imaginary parts, and eliminating the unknown fault resistance (R_{FA}), the sought fault distance (d_{FA}) is determined as:

$$d_{FA} = \frac{\text{real}(\underline{V}_{Ap})\,\text{imag}(\underline{I}_{FA}) - \text{imag}(\underline{V}_{Ap})\,\text{real}(\underline{I}_{FA})}{\text{real}(\underline{Z}_{1LA}\underline{I}_{Ap})\,\text{imag}(\underline{I}_{FA}) - \text{imag}(\underline{Z}_{1LA}\underline{I}_{Ap})\,\text{real}(\underline{I}_{FA})} \tag{6}$$

Having the fault distance calculated (6), the fault resistance R_{FA} can be also determined, as for example as:

$$R_{FA} = \frac{\text{real}(\underline{V}_{Ap}) - d_{FA}\,\text{real}(\underline{Z}_{1LA}\underline{I}_{Ap})}{\text{real}(\underline{I}_{FA})} \tag{7}$$

The distance to fault d_{FA} in (6) is a relative distance for the line section AA–X and can be recalculated to the relative distance for the whole line AA–BA as follows:

$$d_A = d_{FA}\,d_{SC} \tag{8}$$

where d_{SC} – relative distance from the bus AA to SCs&MOVs.

III. Fault Location Subroutine SUB_B

In the case of subroutine SUB_B (Fig. 4) the fault locator FL_B can fulfill its duty by considering the fault loop seen from the bus BA, i.e. containing the line section from the bus BA up to the fault FB and fault path resistance R_{FB}. Analogously as for the sub-routine SUB_A, there is no need for representing the SCs&MOVs in the considered fault loop. The generalized fault model for such fault loop is formulated as in (1), but with utilizing the signals from the line terminals BA&BB.

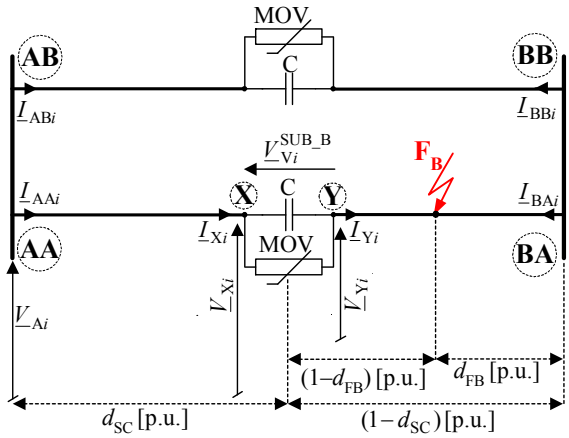

Fig. 4. Scheme for subroutine SUB_B (for fault FB)

The distance to fault d_{FB} marked in Fig. 6 is a relative distance for the line section BA–Y and can be recalculated to the relative distance for the whole line BA–AA as follows:

$$d_B = d_{FB}(1 - d_{SC}) \tag{9}$$

where $(1–d_{SC})$ – relative distance from the bus BA to SCs&MOVs.

IV. Selection Unit

The applied subroutines SUB_A, SUB_B yield the results for a distance to fault and fault resistance: (d_A, R_{FA}); (d_B, R_{FB}), respectively. The results from only one subroutine (the valid one) are consistent with the actual fault. First, the subroutine yielding the distance to fault outside the section range and/or

the fault resistance of negative value is rejected. If this is insufficient, then one has to continue the selection.

It is proposed to base the further selection step on estimation of the resistance and reactance for the fundamental frequency equivalent of the compensating bank [2], [5]. This estimation has to be carried out for both subroutines (SUB_A and SUB_B). For this purpose the fault locator FL_A determines the following auxiliary impedances:

$$\underline{Z}_{\mathrm{Xph}}^{\mathrm{SUB\_A}} = \frac{\underline{V}_{\mathrm{Xph}}^{\mathrm{SUB\_A}}}{\underline{I}_{\mathrm{BAph}}}, \qquad \underline{Z}_{\mathrm{Xph}}^{\mathrm{SUB\_B}} = \frac{\underline{V}_{\mathrm{Xph}}^{\mathrm{SUB\_B}}}{\underline{I}_{\mathrm{AAph}}} \tag{10}$$

where: $\underline{V}_{\mathrm{Xph}}^{\mathrm{SUB\_A}}$, $\underline{V}_{\mathrm{Xph}}^{\mathrm{SUB\_B}}$ – voltages at the point X from any of the faulted phases (phase: ph), determined according to Fig. 3 (SUB_A) and Fig. 4 (SUB_B); $\underline{I}_{\mathrm{BAph}}$, $\underline{I}_{\mathrm{AAph}}$ – currents at the line ends BA and AA from the faulted phase (ph), which after neglecting the line shunt capacitances are equal to currents at the capacitor bank.

The fault locator FL_B determines the auxiliary impedances:

$$\underline{Z}_{\mathrm{Yph}}^{\mathrm{SUB\_A}} = \frac{\underline{V}_{\mathrm{Yph}}^{\mathrm{SUB\_A}}}{\underline{I}_{\mathrm{BAph}}}, \qquad \underline{Z}_{\mathrm{Yph}}^{\mathrm{SUB\_B}} = \frac{\underline{V}_{\mathrm{Yph}}^{\mathrm{SUB\_B}}}{\underline{I}_{\mathrm{AAph}}} \tag{11}$$

where: $\underline{V}_{\mathrm{Yph}}^{\mathrm{SUB\_A}}$, $\underline{V}_{\mathrm{Yph}}^{\mathrm{SUB\_B}}$ – voltages as in (10), but at the point Y (Figs. 3 and 4), $\underline{I}_{\mathrm{BAph}}$, $\underline{I}_{\mathrm{AAph}}$ – currents as in calculations according to (10).

In order to calculate the voltages used for determining the auxiliary impedances (10)–(11) one has to start with the analytic transfer of voltages from the line terminals to the points X, Y, for the respective sequences [5]. Then, the sequence voltages are to be transferred to the phase domain in order to get the voltages from the faulted phase (in case of multi-phase faults one takes any phase from those involved in a fault). This is so since the judgment with respect to which subroutine is valid can be performed by considering the character of the estimated fundamental frequency impedance of the compensating bank from any of the faulted phases:

$$\underline{Z}_{\mathrm{Vph}}^{\mathrm{SUB\_A}} = \underline{Z}_{\mathrm{Yph}}^{\mathrm{SUB\_A}} - \underline{Z}_{\mathrm{Xph}}^{\mathrm{SUB\_A}} \tag{12}$$

$$\underline{Z}_{\mathrm{Vph}}^{\mathrm{SUB\_B}} = \underline{Z}_{\mathrm{Xph}}^{\mathrm{SUB\_B}} - \underline{Z}_{\mathrm{Yph}}^{\mathrm{SUB\_B}} \tag{13}$$

Thus, determination of the impedances (12)–(13) requires only subtracting the auxiliary impedances determined by the fault locators FL_A and FL_B (Fig. 2). The subroutine which yields the estimated impedance of the series *R*–*C* circuit character (resistance>0 and reactance<0) [2], with the parameters from the expected range, is selected as the valid subroutine. It has been checked for huge number of fault cases that the expected range for the resistance and reactance of the compensating bank impedance is even not needed (see the example in Section V).

V. ATP-EMTP Based Testing of the Fault Location Algorithm

The 300-km, 400-kV transmission line compensated in the middle (d_{SC}=0.5 p.u.), at the degree of 70%, was modeled using ATP-EMTP software [9]. The line impedances and capacitances for particular sequences were assumed as:
$\underline{Z}_{1L}$=(8.28+j94.5) Ω, $\underline{Z}_{0L}$=(82.5+j307.9) Ω, $\underline{Z}_{0m}$=(63+188.5) Ω,
C_{1L}=13 nF/km, C_{0L}=8.5 nF/km, C_{0m}=5 nF/km.

The supplying systems A and B (Fig. 2) were modeled taking for them the following impedance values: $\underline{Z}_{1SA}$=$\underline{Z}_{1SB}$=(1.31+j15) Ω, $\underline{Z}_{0SA}$=$\underline{Z}_{0SB}$=(2.32+j26.5) Ω; the e.m.f. of the system B as delayed by 30° with respect to the system A.

The MOVs with the common approximation:

$$i = P\left(\frac{v}{V_{\mathrm{REF}}}\right)^{q} \tag{14}$$

were modeled taking: P=1 kA, V_{REF}=150 kV, q=23.

The model includes the Capacitive Voltage Transformers (CVTs) and the Current Transformers (CTs). The analog filters with 350 Hz cut-off frequency were also included. The sampling frequency of 1000 Hz was applied and the phasors were determined with use of the DFT algorithm.

In Figs. 5 through 7 the results for the example fault location are presented. The specifications for the presented example are:
- fault type: a-g,
- fault location: d_{B_actual}=0.3 p.u. (i.e. on the section BA–Y at 90 km from the bus BA),
- fault resistance: R_{FB}=25 Ω.

Three-phase voltage from two ends of the line and three-phase currents from both line circuits and from two line ends are shown in Fig. 5. In turn, Fig. 6 presents estimated fault distances (d_A, d_B – determined according to (8)–(9)) and fault resistances (R_{FA}, R_{FB}) for the both subroutines SUB_A, SUB_B. Both locators (FL_A, FL_B) determine the fault position as within their sections and fault resistances of positive real numbers:
- FL_A: d_{A_mean}=0.4935 p.u. (<d_{SC}); R_{FA_mean}=47.2 Ω,
- FL_B: d_{B_mean}=0.3006 p.u. (<(1–d_{SC})); R_{FB_mean}=24.3 Ω.

Note: 'mean' in the subscripts of the above results denote the mean values of the estimated quantities from the interval of 30 to 50 ms of the fault time.

Having only the results for the fault distance and fault resistance from both fault locators FL_A and FL_B a dilemma which fault locator yields the valid results, i.e. the results consistent with the actual fault, arises. This dilemma can be resolved by estimating the fundamental frequency equivalent impedance for the compensating bank. The mean resistance and reactance for this impedance in the faulted phase 'a' – relevant for the subroutines SUB_A (12) and SUB_B (13), as presented in Fig. 7, are:

- SUB_A: $\left(\underline{Z}_{Vph}^{SUB\_A}\right)_{mean} = (-29.88 - 63.08\mathrm{i})\,\Omega$,

- SUB_B: $\left(\underline{Z}_{Vph}^{SUB\_B}\right)_{mean} = (20.10 - 46.11\mathrm{i})\,\Omega$.

For the subroutine SUB_B we get a realistic result (the determined impedance has the character of *R*–*C* circuit) while the subroutine SUB_A has to be rejected as the false one (the determined impedance is of evidently negative resistance).

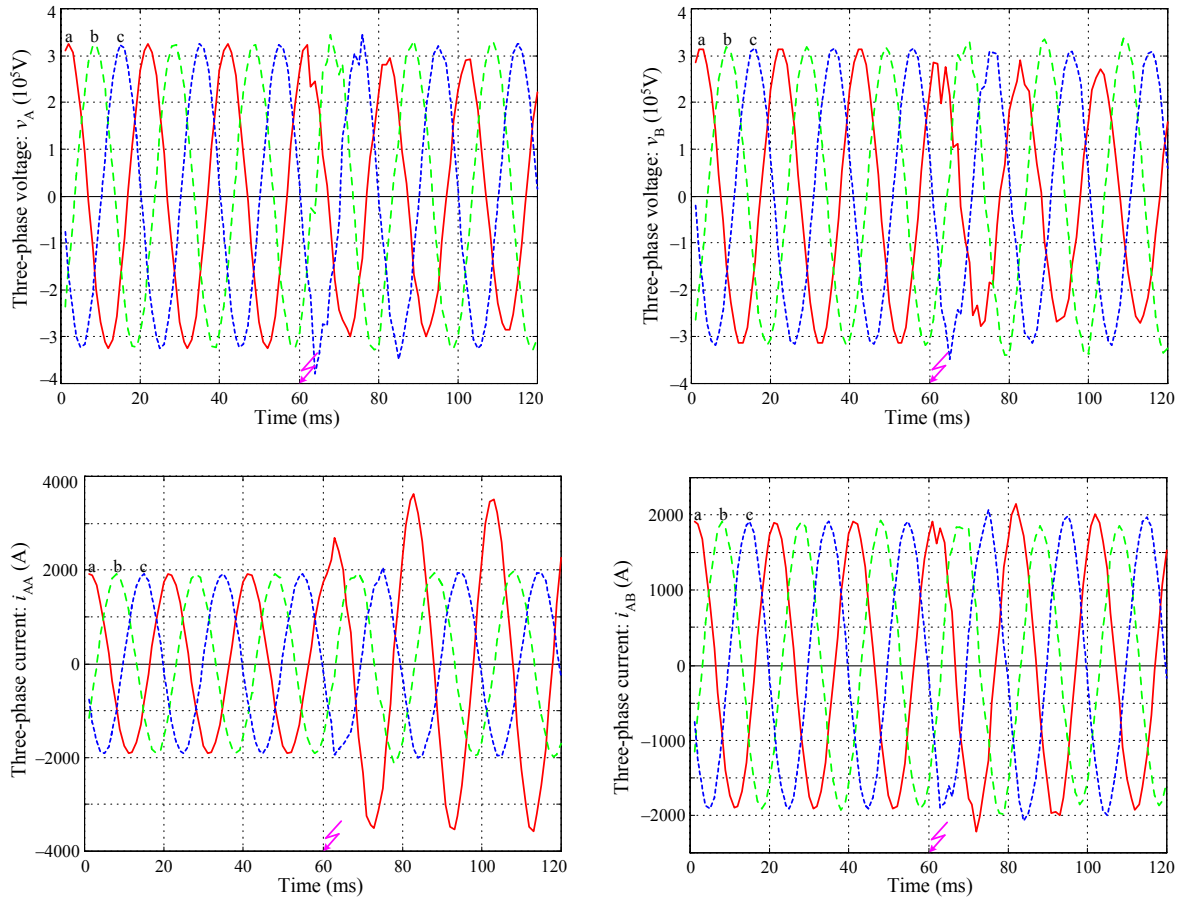

(Fig. 5 to be continued)

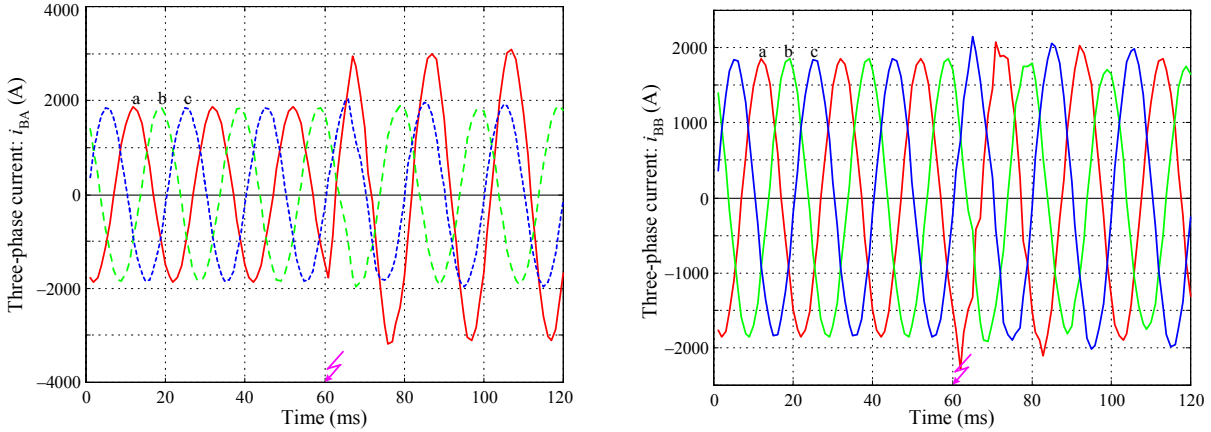

Fig. 5. The example – three-phase voltages and currents from both ends of the faulted double-circuit test line

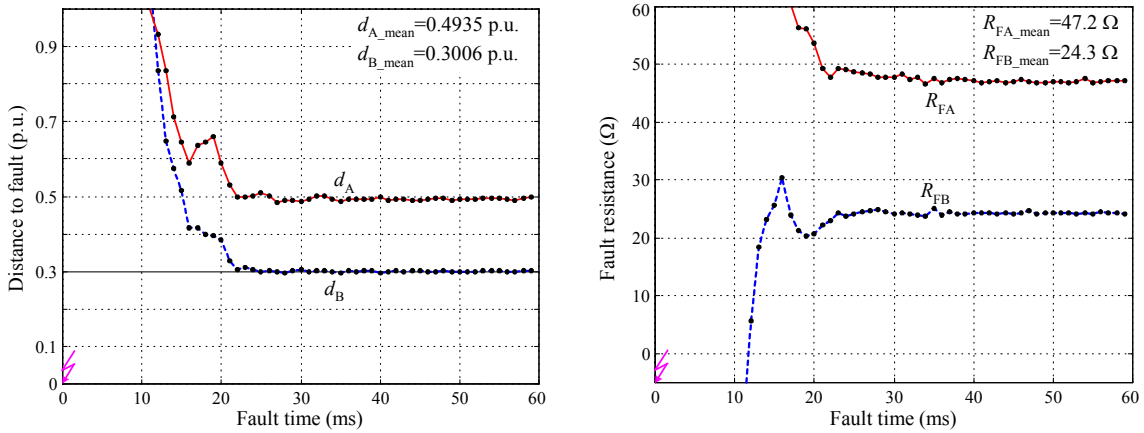

Fig. 6. The example – estimated distance to fault and fault resistance according to subroutines SUB_A, SUB_B

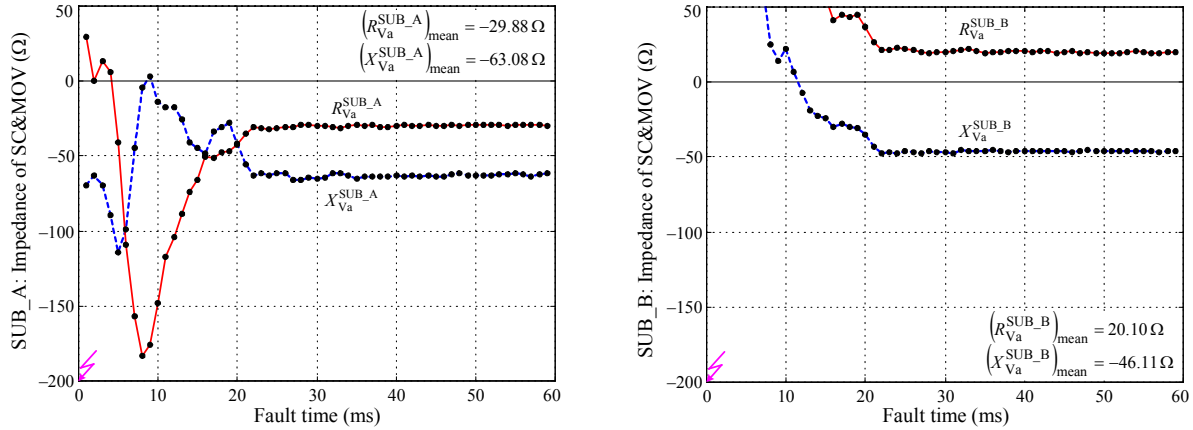

Fig. 7. The example – selection of valid subroutine: SUB_A (false subroutine), SUB_B (valid subroutine)

The valid subroutine SUB_B yields the fault distance: d_{B_mean}=0.3006 p.u. Thus, fault location in this example is performed with small error (equal to 0.06%). Different specifications of faults and pre-fault power flows have been considered in the evaluation of the accuracy of the developed fault location algorithm. For the faults involving fault resistance up to 30 Ω, the maximum errors do not exceed: 0.35% for the case of the instrument transformers with ideal transformation and 1% with the real instrument transformers included. Such errors are definitely acceptable for practical applications.

VI. CONCLUSIONS

The presented fault location method can be easily accomplished by embedding fault locators into current differential protective relays of a single- or double-circuit series-compensated line. In this way a communication infrastructure of differential relays is utilized and thus additional communication links are not demanded. Moreover, functionality of a differential relay is greatly increased.

A single fault locator or two locators at both line ends can be applied. The latter method as not involving the parameters of the compensating bank in fault calculations allows for achieving better fault location accuracy.

The derived selection procedure allows reliable indication of the subroutine results, which are consistent with the actual fault.

In the presented considerations, the double-circuit line under study was represented using the lumped parameter line model. This is justified when, as it was considered, the capacitor compensating bank is installed in midpoint of the line dividing it into two segments of the moderate length.

The presented fault location technique has been thoroughly tested using signals taken from ATP-EMTP versatile simulations of faults on a test double-circuit transmission line with capacitor compensation. The presented example and the carried out through evaluation show the validity and high accuracy of the developed fault location technique.

VII. REFERENCES

[1] IEEE Std C37.114: IEEE Guide for Determining Fault Location on AC Transmission and Distribution Lines, IEEE Power Engineering Society Publ., 8 June 2005: 1-42

[2] Saha MM, Izykowski J, Rosolowski E and Kasztenny B, A new accurate fault locating algorithm for series compensated lines. IEEE Trans. on Power Delivery, 1999, Vol. 14, No. 3: 789-797

[3] Yu C-S, Liu C-W, Yu S-L and J-A Jiang J-A, A new PMU-based fault location algorithm for series compensated lines. IEEE Trans. on Power Delivery, 2002, Vol. 17, No. 1: pp. 33-46

[4] Fecteau C, Accurate fault location algorithm for series compensated lines using two-terminal unsynchronised measurements and Hydro-Quebec's field experience. In: Proceedings of 33-rd Annual Western Protective Relay Conference, Spokane, 2006: 1-16

[5] Saha MM, Izykowski J and Rosolowski E, A fault location method for application with current differential protective relays of series-compensated transmission line. In: Proceedings of 10th IET Conference on DPSP, 29.03-01.04.2010, paper 05.2

[6] Evrenosoglu CY and Abur A, Fault location for teed circuits with mutually coupled lines and series capacitors. In: Proceedings of IEEE Bologna Power Tech Conference, 2003, IEEE Catalog Number 03EX719C

[7] Cheong WJ and Aggarwal RK, A novel fault location technique based on current signals only for thyristor controlled series compensated transmission lines using wavelet analysis and self-organising map neural networks. In: Proceedings of 8-th IEE Conference on DPSP, Vol. 1, 2004: 224-227

[8] Saha MM, Izykowski J and Rosolowski E, Fault Location on Power Networks, Springer, London, 2010

[9] Dommel H, ElectroMagnetic Transients Program, BPA, Portland, Oregon, 1986.